行政院國家科會委員專題研究計畫報告

共軛有機聚合物的電子光譜與光致電子轉移

計畫編號：NSC-89-2113-M002-056

計畫主持人 金必耀 教授

處理方式：可立即對外提供參考

執行單位：台灣大學化學系

中華民國九十一年二月

行政院國家科會委員專題研究計畫報告

共軛有機聚合物的電子光譜與光致電子轉移
Lattice Relaxation Theory of Photoinduced Charge Transfer in a Molecularly Doped Conjugated Polymer

楊定學(Ding-Shyue Yang)，金必耀(Bih-Yaw Jin)
台灣大學化學系

計畫編號： NSC-89-2113-M002-056

Abstract

Lattice relaxation is considered in our theoretical study of ultrafast photoinduced charge transfer in a molecularly doped conducting polymer. Under the constraint of single excitation, simplification of differential overlaps and the assumption of electron-hole symmetry, a full microscopic Hamiltonian for the composite system is derived and inspected. With the incorporation of electron-phonon coupling, which is treated site-off-diagonally, and through self-consistent-field calculation we acquire the electronic properties and lattice configurations of the initial and final states in the charge-transfer process. Charge localization may occur in the excitonic and charge-transfer bound states due to stronger lattice relaxation, while the charge-transfer continuum still show delocalized properties. By using Fermi's golden rule and Huang-Rhys factors we find that the decay between two bound states is most efficient, and its rate exceeds other routes' by about two orders of magnitude. In our theory, the charge transfer can take place on a picosecond, even a subpicosecond time scale, which agrees with many recent experimental results.

1 Introduction

Photoinduced charge transfer in conducting polymers has been a central issue since some photophysical properties of conjugated polymers doped with fullerene molecules C_{60} were reported.[1, 2]. Subsequently in one decade, not only the fundamental interest in the excited states and their photophysics[3, 4, 5, 6, 7, 8, 9, 10, 11] but the potential applications to photodiodes, photovoltaic cells and artificial photosynthesis[12, 13, 14, 15, 16] make the studies of photoinduced charge transfer intriguing and noticeable. To understand this photogeneration process, Rice and Gartstein[17] suggested a purely electronic microscopic model, and supposed that for energy being conserved, two kinds of weak perturbations connects the initial exciton state with the continuum part of the charge-transfer excitation spectrum. After numerical calculations with their choices for the parameters, they estimated that the decay rate might be as large as 10^{12} s^{-1}, as observed in many experiments.[1, 4, 3, 7, 9] However, since an available continuum of band excitation in the final state is necessary, the polymer chain should be of infinite (or finite but very long) length; for finite chains or conjugation lengths, vibronic coupling to broaden the molecular orbital levels must be considered. Moreover, although it is true for very dilute systems, the linear dependence of the charge-transfer rate on the dopant concentration factor $c = N_d/N$ disappear for highly-doped conducting polymers.[11] Now that electron-phonon coupling may be an important issue on a one-dimensional deformable lattice, we want to incorporate the effects of lattice relaxation into our microscopic model.

In this paper, we present a lattice relaxation theory of the photoinduced charge transfer in such conjugated polymer/dopant composites. Similar to the previous model,[17] two relevant electron-hole excitation spectra are concerned with our model. Before the charge transfer, the electron-hole excitations are photoinduced on conducting polymers regardless of the presence of dopant molecules and form the intrapolymer spectrum. We assume that relaxation to the lowest excitation happens and the equilibrium of its phonon part achieves much more rapidly than the time scale of the charge transfer, thus this exciton state serves as the initial state of our theory. The other spectrum describes the energies of excitations corresponding to one charge moving from the polymer onto an adjacent molecule in the presence of another charge of opposite sign, and therefore it can be referred as the charge-transfer spectrum. On the dopant an acceptor level at the energy

Δ relative to the center of the polymer's energy gap is considered. In order to make the photoinduced charge transfer possible, under the constraint of energy conservation Δ must satisfy the following inequality

$$-E_{polymer,CT1} \leq \Delta \leq E_{EX} - E_{polymer,CT1}, \tag{1}$$

where E_{EX} is the lowest energy of the intrapolymer spectrum and $E_{polymer,CT1}$ is the energy of the polymer of the lowest charge-transfer state, i.e. $E_{polymer,CT1} + \Delta = E_{CT1}$. In Eq. (1) the left inequality eliminates the possibility of a spontaneous charge-transfer process ($E_{CT1} < 0$), and the right inequality guarantee the decay path is energetically favored ($E_{EX} \geq E_{CT1}$). Compared with the previous research,[17] decay from the initial state to the lowest excitation of the charge-transfer spectrum can be considered readily, which will later be shown as the fastest charge-transfer way that can be found in this extrinsic photoconductor, even exceeding all the other possible routes by about two orders of magnitude. A diagrammatic representation of the system and the decay processes is illustrated in Fig. 1.

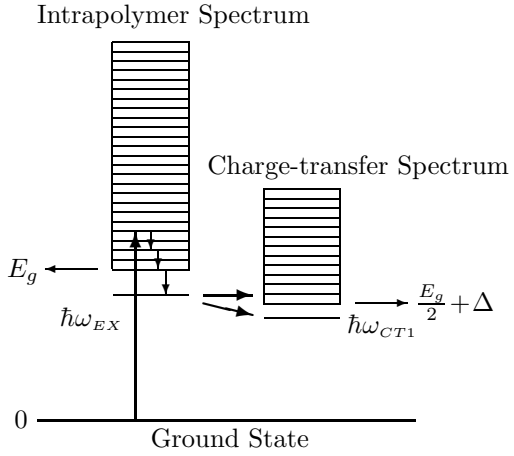

Figure 1: Diagrammatic representation of the intrapolymer and charge-transfer electron-hole excitation spectra (with the electronic parts shown only) and some possible paths of charge transfer. The criterion of energy conservation is held by a number of phonons being excited.

In Sec. 2 a model Hamiltonian suitable for the study of the polymer/molecule composite is carefully deduced and examined under several assumptions and the constraint of single excitation. we indicate that two terms of the electron-hole interaction $\mathcal{H}_{e-h}$ and a new mechanism of charge transfer $\mathcal{V}_3$, named as the exciton-to-charge-transfer-exciton process, can only function in a singlet state. Although we will not discuss triplet states in this paper and therefore the effects of these terms will be integrated into those of equal virtue, they may play an important role in the study of the difference between the recombination rates of singlet and triplet excitations. Then in Sec. 3 lattice relaxation is incorporated into the model Hamiltonian, and detailed calculation strategies of the states, the lattice configurations and charge-transfer rates are described. We deal with the lattice part of the system classically with the electron-phonon coupling terms appearing off-diagonally in the Hamiltonian matrix, which may be categorized as the branch of acoustic phonons. The central idea of this paper is that we can utilize Huang-Rhys factors under short-time approximation, the strong-coupling scheme and high-temperature limit for the lattice system consisting of displaced oscillators[18, 19], and Fermi's golden rule to calculate the charge-transfer rate. Therefore in Sec. 4 the effects of different settings of parameters are discussed specifically for the energies of the spectra, the wavefunctions, lattice deformation and the analyses of normal modes. The legitimacy of our methods is also verified. By calculating Huang-Rhys factors, we show that decay of a polymer exciton may be as fast as in a subpicosecond time scale, which is in agreement with the experimental observations, thus the effect of lattice relaxation is taken into consideration successfully.

2 Hamiltonian of the Composite System

We simplify a molecularly doped conjugated polymer as a composite of a single straight polymer chain with N unit cells and a single dopant molecule placed adjacent to the jth unit. For each unit cell two representative localized wavefunctions, e.g. orthonormalized HOMO and LUMO or two Wannier functions localized at it, corresponding to the valence and conduction bands respectively, are taken into account in our microscopic model. On the dopant molecule we shall consider a dominant electron-acceptor level which only interacts slightly with the adjacent polymer site (for the case of hole transfer our model is also valid with some slight modifications). Then these localized spin orbitals, constructed to be an orthonormal basis set, may be written as

$$\begin{aligned}
\mathcal{W}^{\sigma}_{lV}(\chi) &\equiv \mathcal{W}_{V}(\mathbf{r}-\mathbf{l})\cdot\sigma,\\
\mathcal{W}^{\sigma}_{lC}(\chi) &\equiv \mathcal{W}_{C}(\mathbf{r}-\mathbf{l})\cdot\sigma,\\
\mathcal{W}^{\sigma}_{jD}(\chi) &\equiv \psi_{D}(\mathbf{r}-\mathbf{d})\cdot\sigma.
\end{aligned}$$

Following the formalism of second quantization[20, 21], the field operator $\psi(\chi)$ can be defined by

$$\psi(\chi)=\sum_{l,\sigma} a_{l\sigma V}\mathcal{W}^{\sigma}_{lV}(\chi)+\sum_{l,\sigma} a_{l\sigma C}\mathcal{W}^{\sigma}_{lC}(\chi)+\sum_{\sigma} a_{j\sigma D}\mathcal{W}^{\sigma}_{jD}(\chi), \tag{2}$$

where $a_{l\sigma V}$, $a_{l\sigma C}$, and $a_{j\sigma D}$ are fermion operators, which annihilate, respectively, an electron with spin polarization σ in the localized wavefunctions belonging to the valence band, the conduction band (centered at the lth unit cell), and the acceptor level of the dopant molecule. We will use Eq. (2) to build the effective Hamiltonian of the composite system.

Basically, there are nine different terms in the one-particle part of total Hamiltonian: three of them are number operators representing the energy of a single electron in some energy band or the acceptor level, while the other six describe the transfers between energy bands and the acceptor level under the operation of one-particle Hamiltonian, consisting of the kinetic energy part and the potential energy of lattice $V_L(\mathbf{r})$. Because our interest mainly focuses on photoinduced charge transfer between the conducting polymer and the dopant molecule, transfers directly from the valence band to the dopant will not be considered. Besides, we assume that this part of Hamiltonian will not cause charge transfer between the valence and conduction bands. Therefore the single-particle Hamiltonian is given by

$$\begin{aligned}
\mathcal{H}_S &= \sum_{l,m,\sigma} a^{\dagger}_{l\sigma V}a_{m\sigma V}H^{VV}_{lm}+\sum_{l,m,\sigma} a^{\dagger}_{l\sigma C}a_{m\sigma C}H^{CC}_{lm}\\
&+\sum_{\sigma} a^{\dagger}_{j\sigma D}a_{j\sigma D}H^{DD}_{jj}+\left(\sum_{l,\sigma} a^{\dagger}_{l\sigma C}a_{j\sigma D}H^{CD}_{lj}+h.c.\right),
\end{aligned} \tag{3}$$

where the matrix element $H^{\xi\eta}_{lm}$ is

$$H^{\xi\eta}_{lm}=\int \mathcal{W}^{*}_{l\xi}(\mathbf{r})\left\{-\frac{\hbar^2}{2m}\nabla^2+V_L(\mathbf{r})\right\}\mathcal{W}_{m\eta}(\mathbf{r})\,d^3r.$$

Now we investigate the two-particle part of total Hamiltonian. In principle there are 81 different terms, too many to be readily handled, so it is necessary to adopt some approximations in our model. First, similar to the consideration of Pariser-Parr-Pople (PPP) method, neglect of differential overlaps between different unit cells and between the dopant and non-adjacent sites will be introduced. Second, only single excitation will be considered, thus successively creating or annihilating two electrons in the valence band, in the conduction band or on the dopant is excluded from the Hamiltonian. Now we are able to reduce the 81 different terms to just 18 ones after collecting and combining each equivalent pair of the remaining terms. Then we effect the particle-hole transformation by introducing the following fermion operators

$$b^{\dagger}_{l,-\sigma}\equiv a_{l\sigma V}\qquad a_{l\sigma}\equiv a_{l\sigma C}\qquad d_{j\sigma}\equiv a_{j\sigma D},$$

which represent, respectively, the creation of a hole in the valence band, the annihilation of an electron in the conduction band, and the annihilation of an electron in the acceptor level of the dopant relative to the Fermi level. After rewriting the 18 terms in the notation defined above, we further assume electron-hole symmetry, eliminating the terms in which the number of creation operators is not equal to that of annihilation operators. Finally, only 8 different terms are to be considered in our model, and by using the anticommutation relations of fermion operators we may categorize the full Hamiltonian of the polymer/dopant composite into 7 different parts: $\mathcal{H} \equiv \mathcal{H}_C^{eff} + \mathcal{H}_h + \mathcal{H}_D + \mathcal{H}_{e-h} + V_1 + V_2 + V_3$.

We first collect those summations only related to the conduction band to be the effective Hamiltonian for the electron space $\mathcal{H}_C^{eff}$ given by

$$\mathcal{H}_C^{eff} \equiv \sum_{l,m,\sigma} a_{l\sigma}^\dagger a_{m\sigma} H_{lm}^{CC} + \sum_{l,\sigma} a_{l\sigma}^\dagger a_{l\sigma} \times$$

$$\underbrace{\left(\sum_{m,s} \left\langle w_{mV} w_{lC} \middle| w_{lC} w_{mV} \right\rangle - \left\langle w_{lC} w_{lV} \middle| w_{lC} w_{lV} \right\rangle \right)}_{\Delta E_C} \tag{4}$$

$$= \sum_{l,\sigma} a_{l\sigma}^\dagger a_{l\sigma} \left(H_{ll}^{CC} + \Delta E_C \right) + \sum_{l \neq m,\sigma} a_{l\sigma}^\dagger a_{m\sigma} H_{lm}^{CC}, \tag{5}$$

where the two-electron integral $\left\langle w_{l_1\xi_1} w_{l_2\xi_2} \middle| w_{l_3\xi_3} w_{l_4\xi_4} \right\rangle$ is given as

$$\int\int d^3r' d^3r \; w_{\xi_1}^*(\mathbf{r} - \mathbf{l_1}) w_{\xi_2}^*(\mathbf{r}' - \mathbf{l_2}) \times \frac{e^2}{|\mathbf{r} - \mathbf{r}'|} w_{\xi_3}(\mathbf{r}' - \mathbf{l_3}) w_{\xi_4}(\mathbf{r} - \mathbf{l_4}). \tag{6}$$

From Eq. (4) it is clearly seen that ΔE_C, which can be easily shown as a constant by change of variables in Eq. (6), consists of Coulomb integrals between the valence- and conduction-band wavefunctions and the exchange integral in the same unit cell, and in Eq. (5) the first summation represents the energy of an electron in a unit cell and the second describes the hopping of an electron between two different sites. If the potential energy of lattice $V_L(\mathbf{r})$ is also periodic, each coefficient may further be parametrized in a simple form, e.g. Hückel-type or PPP-type form.

Similarly we can define the Hamiltonian for the hole space by

$$\mathcal{H}_h \equiv -\sum_{l,\sigma} b_{l\sigma}^\dagger b_{l\sigma} H_{ll}^{VV} - \sum_{l \neq m,\sigma} b_{m\sigma}^\dagger b_{l\sigma} H_{lm}^{VV} + \sum_{l,\sigma} H_{ll}^{VV}.$$

The constant shift $\sum_{l,\sigma} H_{ll}^{VV}$ rises from the energy of all the electrons in the valence band, while the first two terms, like those in Eq. (5), represent the energy of a hole in a unit cell and the hopping of a hole between two different sites, respectively. The Hamiltonian for the dopant molecule can also be defined by

$$\mathcal{H}_D \equiv \sum_{\sigma} d_{j\sigma}^\dagger d_{j\sigma} \left(H_{jj}^{DD} + \sum_{l,s} \left\langle w_{lV} w_{jD} \middle| w_{jD} w_{lV} \right\rangle - \left\langle w_{jD} w_{jV} \middle| w_{jD} w_{jV} \right\rangle \right),$$

where the coefficient in the parentheses, the energy of an electron in the acceptor level of the molecule ΔE_D, may also be shown as another constant with the contribution of Coulomb integrals with the full electron pool and the exchange integral between the dopant and the nearest neighbor.

Then the Hamiltonian describing interaction between electrons and holes can be explicitly written as

$$\begin{aligned}
\mathcal{H}_{e-h} \equiv \; & - \sum_{l,m,\sigma,s} a_{ms}^\dagger a_{ms} b_{l\sigma}^\dagger b_{l\sigma} \left\langle w_{lV} w_{mC} \middle| w_{mC} w_{lV} \right\rangle \\
& + \sum_{l,m,\sigma,s} a_{l\sigma}^\dagger b_{l,-\sigma}^\dagger b_{m,-s} a_{ms} \left\langle w_{lC} w_{mV} \middle| w_{mC} w_{lV} \right\rangle \\
& - \sum_{l,\sigma,s} d_{js}^\dagger d_{js} b_{l\sigma}^\dagger b_{l\sigma} \left\langle w_{lV} w_{jD} \middle| w_{jD} w_{lV} \right\rangle \\
& + \sum_{\sigma,s} d_{j\sigma}^\dagger b_{j,-\sigma}^\dagger b_{j,-s} d_{js} \left\langle w_{jD} w_{jV} \middle| w_{jD} w_{jV} \right\rangle .
\end{aligned} \tag{7}$$

From the viewpoint of coefficients the first and third terms are Coulomb integrals, and the second and fourth terms are exchange integrals between an electron and a hole; however, from the viewpoint of operators, the second and fourth terms may be interpreted as the migration of an electron-hole pair, i.e. the combination and regeneration of an exciton in the mth and lth unit cells, respectively. For example, if we define $B^{\dagger}_{l,\sigma} \equiv a^{\dagger}_{l\sigma} b^{\dagger}_{l,-\sigma}$, operators of the second term $a^{\dagger}_{l\sigma} b^{\dagger}_{l,-\sigma} b_{m,-s} a_{ms}$ will be $B^{\dagger}_{l\sigma} B_{ms}$, the transfer of singlet excitation between two unit cells. Therefore, only singlet states will be affected by these two terms in $\mathcal{H}_{e-h}$, and the spectrum of triplet states may be different from the (singlet) intrapolymer spectrum described previously. We hereon define $\mathcal{H}_0$ to describe the energy of the intrapolymer and charge-transfer excitations of the composite system by the Hamiltonian

$$\mathcal{H}_0 \equiv \mathcal{H}_C^{eff} + \mathcal{H}_h + \mathcal{H}_D + \mathcal{H}_{e-h}. \tag{8}$$

Three different mechanisms of the photoinduced charge-transfer process may be inferred from our microscopic models. First, the single-particle hopping process $\mathcal{V}_1$ can be described by the Hamiltonian

$$\begin{aligned} \mathcal{V}_1 \equiv \quad & \sum_{l,\sigma} d^{\dagger}_{j\sigma} a_{l\sigma} H^{DC}_{jl} + \sum_{\sigma} d^{\dagger}_{j\sigma} a_{j\sigma} \times \\ & \underbrace{\left(\sum_{l,s} \left\langle w_{lV} w_{jD} \middle| w_{jC} w_{lV} \right\rangle - \left\langle w_{jD} w_{jV} \middle| w_{jC} w_{jV} \right\rangle \right)}_{V_{C\to D}} \\ & + \quad h.c., \end{aligned} \tag{9}$$

where $V_{C\to D}$ is also a constant, containing the Coulomb and exchange integrals, and the operators show the hop of an electron from the conduction band onto the dopant. Rice and Gartstein[17] restricted this hopping process to occur between the molecule and the adjacent polymer unit cell, neglecting the first term in Eq. (9). Second, the perturbation for the charge-fluctuation charge-transfer process can be defined by

$$\mathcal{V}_2 \equiv - \sum_{l,\sigma,s} d^{\dagger}_{j_s} b^{\dagger}_{l\sigma} b_{l\sigma} a_{j_s} \left\langle w_{jD} w_{lV} \middle| w_{lV} w_{jC} \right\rangle - h.c., \tag{10}$$

where the given name stands for the transfer of an electron from the polymer to the dopant correlated with a local charge fluctuation of the hole density. Now we will propose a new mechanism of the photoinduced charge transfer, called the exciton-to-charge-transfer-exciton process, to be defined by the Hamiltonian

$$\mathcal{V}_3 \equiv \sum_{l,\sigma,s} d^{\dagger}_{j_s} b^{\dagger}_{j,-s} b_{l,-\sigma} a_{l\sigma} \left\langle w_{jD} w_{lV} \middle| w_{lC} w_{jV} \right\rangle + h.c. \tag{11}$$

As indicated by the operators, this process associates with the combination of an exciton in the lth unit cell and the generation of a charge-transfer exciton in the vicinity of the molecule. Since the annihilation and recreation of an exciton in Eq. (11) belong to singlet excitation, the perturbation $\mathcal{V}_3$ will distinguish triplet states from the singlet, which may be important in the case of the decay of an triplet polymer exciton; however, in singlet systems the contribution of $\mathcal{V}_3$ may be integrated into that of $\mathcal{V}_2$, so we will not specifically discuss $\mathcal{V}_3$ in this study.

3 Lattice Relaxation Theory

Now we will take lattice relaxation into account. In order to preserve the orthonormality of the chosen localized wavefunctions and antisymmetric properties of the fermion operators, we assume that lattice deformation is small relative to the size of a unit cell a_0 and it is appropriate to treat the lattice classically. Here two types of linear electron-phonon couplings can be classified: one is the site-diagonal coupling, the on-site correlation between charges and the lattice along the diagonal of the Hamiltonian matrix, and the other is the off-diagonal coupling, the correlation in which different unit cells are involved. In the following discussion

we will focus on the latter type of electron-phonon coupling, and therefore $\mathcal{H}_0$, referring to Eq. (8), can be defined by the Hamiltonian

$$\begin{aligned}\mathcal{H}_0 &= \sum_{n,\sigma}\alpha_0(a^\dagger_{n\sigma}a_{n\sigma}+b^\dagger_{n\sigma}b_{n\sigma})+\sum_{n,\sigma}(t^\circ+\beta(u_{n+1}-u_n))\cdot \\ &\quad \left\{(a^\dagger_{n+1,\sigma}a_{n\sigma}+h.c.)+(b^\dagger_{n+1,\sigma}b_{n\sigma}+h.c.)\right\} \\ &+ \Delta\sum_\sigma d^\dagger_{j\sigma}d_{j\sigma}+\sum_{n,m,\sigma,s}U_{mn}a^\dagger_{ms}a_{ms}b^\dagger_{n\sigma}b_{n\sigma} \\ &+ \sum_{n,\sigma,s}V_{jn}d^\dagger_{js}d_{js}b^\dagger_{n\sigma}b_{n\sigma}+\sum_n\frac{1}{2}K(u_{n+1}-u_n)^2, \end{aligned} \tag{12}$$

where β is the electron-phonon coupling constant, u_n denotes the displacement of the nth site relative to the undistorted lattice, and K is the force constant. In Eq. (12) zero potential energy is set to the center of the polymer's energy gap and electron-hole symmetry is assumed; thus the positive constant α_0 denotes the energy gain of a charge created in a unit cell, the negative constant t° is the resonance integral between adjacent sites, Δ denotes the energy of the acceptor level of the dopant molecule, and U_{mn} and V_{jn} are the effective attractive Coulomb-type interaction between an electron and a hole. Moreover, Coulomb-type interaction can generally be written as

$$V(x,y,z)=-e^2\Big/\sqrt{\epsilon_y\epsilon_z x^2+\epsilon_z\epsilon_x y^2+\epsilon_x\epsilon_y z^2},$$

thus we may take U_{nm} and V_{jn} to be

$$\begin{aligned}U_{nm} &= U\delta_{nm}+(1-\delta_{nm})V\big/ \\ &\quad (|n-m|a_0+sgn(n-m)(u_n-u_m)), \\ V_{jn} &= V\big/\sqrt{d^2+(|j-n|a_0+sgn(j-n)\cdot u_n)^2},\end{aligned}$$

where U is the Coulomb integral within the same site, $V=-e^2\big/\sqrt{\epsilon_y\epsilon_z}$ is the potential energy between an electron and a hole with a unit-length separation, and d denotes the effective distance between the dopant and the polymer chain. Compared with the Hamiltonian proposed formerly,[17] the consideration of lattice relaxation, similar to Su-Schrieffer-Heeger (SSH) model, is appended into our theory with the justification of the Hamiltonian discussed in the last section.

For the intrapolymer electron-hole pair excitation, the two-particle wavefunction of the singlet excitonic bound state can be written as

$$\begin{aligned}|\Psi_{EX}\rangle &= \frac{1}{\sqrt{N}}\sum_{n,m=1}^{N}\Phi_{nm}|\phi_{nm}\rangle \\ &\equiv \frac{1}{\sqrt{2N}}\sum_{n,m=1}^{N}\Phi_{nm}(a^\dagger_{n\alpha}b^\dagger_{m\beta}+a^\dagger_{n\beta}b^\dagger_{m\alpha})|0\rangle,\end{aligned}$$

where $|0\rangle$ denotes the ground-state wavefunction of the composite system and Φ_{nm} is normalized under the constraint $\sum_{n,m=1}^{N}|\Phi_{nm}|^2=N$. The matrix representation of $\mathcal{H}_0$ shows a block-tridiagonal pattern on the basis set $\{|\phi_{nm}\rangle\}$, and the energy of the excitonic bound state is given as

$$\begin{aligned}E_{EX} &\equiv \hbar\omega_{EX}=2\alpha_0+\sum_{n=1}^{N-1}\frac{1}{2}K(\Delta u_{n,EX})^2 \\ &+ \frac{2}{N}\sum_{n=1}^{N-1}\sum_{m=1}^{N}t_n\left(\Phi_{nm}\Phi_{n+1,m}+\Phi_{mn}\Phi_{m,n+1}\right) \\ &+ \frac{1}{N}\sum_{n,m=1}^{N}U_{nm}|\Phi_{nm}|^2,\end{aligned} \tag{13}$$

where $\Delta u_{n,EX}$ is defined to be $(u_{n+1,EX} - u_{n,EX})$. In order to calculate E_{EX}, Φ_{nm} and the lattice conformation, we adopt the following procedures: First, we set the lattice undeformed and fix the center of the polymer lest the unidirectional shift of the whole chain make our calculation diverge, then construct the $\mathcal{H}_0$ matrix, and solve the eigenvalue problem to find the lowest energy and the corresponding probability amplitudes $\{\Phi_{nm}\}$. Next, these amplitudes are substituted into the following equations

$$\begin{aligned} 0 &= \frac{\partial E_{EX}}{\partial(\Delta u_{i,EX})} = K\Delta u_{i,EX} + \frac{1}{N}\sum_{n,m=1}^{N}\frac{\partial U_{nm}}{\partial(\Delta u_{i,EX})}|\Phi_{nm}|^2 \\ &+ \frac{2\beta}{N}\sum_{m=1}^{N}(\Phi_{im}\Phi_{i+1,m} + \Phi_{mi}\Phi_{m,i+1}) \\ &\qquad\qquad \forall\, i = 1, 2, \cdots, N-1 \end{aligned} \tag{14}$$

and Gaussian elimination of order $N-1$ is performed to generate new lattice displacements in equilibrium with the exciton wavefunction. Here adiabatic approximation is assumed, and Eq. (14) is deduced from the generalized Hellmann-Feynman theorem. Then we use the new lattice conformation to build a new $\mathcal{H}_0$ matrix, and repeat these procedures iteratively until the lattice configuration converges within a negligible deviation. Subsequently we analyze the normal modes of the conducting polymer chain by numerically computing the Hessian matrix $\left[\partial^2 E_{EX}/\partial q_i \partial q_j\right]_{N\times N}$ under mass-weighted coordinates $q_{i,EX} \equiv \sqrt{m_i}\; u_{i,EX}$; after diagonalization the eigenvectors are the normal modes, whose frequencies are given by the square roots of their corresponding eigenvalues.

Charge transfer to the dopant molecule may take place after the photoexcitation. The two-particle wavefunction of a singlet charge-transfer state can be written as

$$|\Psi_{CT}\rangle = \sum_{n=1}^{N}\phi_n|\psi_n\rangle \equiv \frac{1}{\sqrt{2}}\sum_{n=1}^{N}\phi_n(d_{j\alpha}^{\dagger}b_{n\beta}^{\dagger} + d_{j\beta}^{\dagger}b_{n\alpha}^{\dagger})|0\rangle,$$

where the probability amplitude ϕ_n indicating the hole in the nth unit cell of the polymer is normalized according to $\sum_{n=1}^{N}|\phi_n|^2 = 1$, and the energy of this state is

$$\begin{aligned} E_{CT} \equiv \hbar\omega_{CT} = \;& \alpha_0 \;\; + \Delta + \sum_{n=1}^{N-1}\frac{1}{2}K(u_{n+1,CT} - u_{n,CT})^2 \\ &+ \sum_{n=1}^{N}V_{jn}|\phi_n|^2 + \sum_{n=1}^{N-1}2t_n\phi_n\phi_{n+1}. \end{aligned} \tag{15}$$

As the iteration procedures of the exciton counterpart, we also take similar strategies to compute the whole charge-transfer spectrum. Notice that it is not needed to fix the center of the polymer chain, for the involvement of the dopant has broken the translational symmetry. The self-consistent-field equation in these states will be

$$\begin{aligned} 0 = \frac{\partial E_{CT}}{\partial u_{i,CT}} &= K(2u_{i,CT} - u_{i+1,CT} - u_{i-1,CT}) \\ &+ \frac{\partial V_{ji}}{\partial u_{i,CT}}|\phi_i|^2 + 2\beta(\phi_{i-1}\phi_i - \phi_i\phi_{i+1}) \\ &\qquad \forall\, i = 2, 3, \cdots, N-1, \end{aligned} \tag{16}$$

and small modifications must be incorporated for the chain ends. Normal-mode analysis will also be done for each charge-transfer state under the mass-weighted coordinates.

After collecting all the information about the excitonic bound state and the charge-transfer states we can use Fermi's golden rule to calculate the decay rate of an intrapolymer exciton in a molecularly doped conjugated polymer,

$$W \equiv \frac{1}{\tau} = \frac{2\pi}{\hbar}\sum_{f}|\langle f|\mathcal{V}_1 + \mathcal{V}_2|i\rangle|^2\delta(E_f - E_i), \tag{17}$$

where $\mathcal{V}_1$ and $\mathcal{V}_2$, as mentioned in the previous section, correspond to the single-particle hopping and the charge-fluctuation charge-transfer processes, respectively. Summation over all charge-transfer states that satisfied the principle of energy conservation is considered. Under Born-Oppenheimer and Condon approximation, we may factorize the matrix element $\langle f|\mathcal{V}_1+\mathcal{V}_2|i\rangle$ into an electronic part and a nuclear part for separate handling. In the nuclear part we assume that the potential well of each normal mode is quadratic such that its behavior can be described by a harmonic oscillator. Besides, after the charge transfer takes place the normal modes of the polymer are retained with small shifts of the equilibrium places at most, i.e. the cases of displaced oscillators $\mathbf{Q}_i^{CTn}=\mathbf{Q}_i^{EX}+\delta_{n_i}$, where n stands for the nth charge-transfer state, i denotes the ith normal mode, and δ_{n_i} represents the displacement of equilibrium. If ω_i is its frequency, we may introduce the Huang-Rhys factor

$$S_{n_i}=\frac{\omega_i\delta_{n_i}^2}{2\hbar}, \tag{18}$$

and under the short-time approximation and the strong-coupling scheme, the charge-transfer rate can be deduced at zero temperature.[18, 19] Moreover, if we take the thermal effect into consideration, under the high-temperature limit, i.e. the assumption that the phonon part of the excitonic bound state reaches its thermal equilibrium very soon after the photoexcitation, the transfer rate can be rederived and written as

$$\begin{aligned} W\equiv\frac{1}{\tau} &= \frac{1}{\hbar^2}\sum_n|\langle\Psi_{CTn}|\mathcal{V}_1+\mathcal{V}_2|\Psi_{EX}\rangle_0|^2 \\ &\times \sqrt{\frac{2\pi}{\sum_i S_{n_i}\omega_i^2 coth\frac{\hbar\omega_i}{2kT}}} \\ &\times exp\left[-\frac{(\omega_{CTn}-\omega_{EX}+\sum_i S_{n_i}\omega_i)^2}{2\sum_i S_{n_i}\omega_i^2 coth\frac{\hbar\omega_i}{2kT}}\right]. \end{aligned} \tag{19}$$

In the electronic part point interaction will be considered; that is, only the localized functions of the unit cells nearest to the dopant molecule will overlap acceptor level. If the number of sites N is even and the molecule is located symmetrically to both chain ends ($j=(N+1)/2$), we may explicitly write down the matrix elements shown in Eq. (19) as

$$\langle\Psi_{CTi}|\mathcal{V}_1|\Psi_{EX}\rangle=\frac{h_0}{\sqrt{N}}\sum_{n=1}^{N}\phi_{ni}\left(\Phi_{\frac{N}{2}n}+\Phi_{\frac{N}{2}+1,n}\right), \tag{20}$$

$$\langle\Psi_{CTi}|\mathcal{V}_2|\Psi_{EX}\rangle=\frac{v_0}{\sqrt{N}}\left(\phi_{\frac{N}{2}i}\Phi_{\frac{N}{2}\frac{N}{2}}+\phi_{\frac{N}{2}+1,i}\Phi_{\frac{N}{2}+1,\frac{N}{2}+1}\right), \tag{21}$$

thus establish the decay rate of an intrapolymer exciton.

4 Calculations and Results

Since there are many parameters in our microscopic model, some of them will be given a constant corresponding to the information of poly(p-phenylenevinylene). We take $a_0=6.5$ Å, $\alpha_0=3.5$ eV, $t^\circ=-1$ eV, the mass of an intermediary (chain-end) unit cell as that of C_8H_6 (C_8H_7), and the dopant molecule to be located at the symmetric position, $j=(N+1)/2$. The energy of the acceptor level Δ need not be considered until the computation of the charge-transfer rate, for it just appears in every diagonal element in the calculation of the charge-transfer spectrum and contributes a constant shift to the overall system energy. All the other adjustable parameters, including the number of unit cells N, the electron-phonon coupling constant β, the on-site electron-hole Coulomb integral U, the relative ratio for electron-hole interaction $U/(V/a_0)$, the effective distance between the molecule and the polymer d, and the force constant of the lattice K, are given numbers summarized in Table 1. Within the range of our parameter set, we consider different degrees of electron-phonon coupling, the rigidity of the lattice, and the two-particle interaction in the composite system to study their influences on the photoinduced charge transfer. During the self-consistent calculations of the intrapolymer and the charge-transfer spectra, computational results will meet the criteria

Table 1: The settings of the parameters in this paper.

β (eV/Å)	U (eV)	$\frac{U}{V/a_0}$	d (Å)	K (eV/Å^2)
0	-0.5	2	2.5	1
0.01	-1	4	5	2.5
0.05	-2		7.5	5
0.1			10	10
0.4				

of convergence and the iterations will be stopped after the maximum displacement of a unit cell is smaller than 10^{-6} Å. In addition, we set 10^{-4} Å as the finite difference of lattice deformation to numerically build the Hessian matrices. Generally, the self-consistency is achieved after several cycles of iterations, and the optimized relaxed geometry of the composite system is indeed a minimum by checking the positivity of the Hessian matrices.

4.1 The Excitonic Bound States

Without electron-phonon coupling, many states whose excitation energy costs are lower than those needed for the band-to-band transitions, about 3 to 12 such bound states generated in a polymer of 30 unit cells, can purely result from the consideration of electron-hole interaction. At this time, the stronger Coulomb interaction U between charges, the more capability it can bind an electron-hole pair to form an energy-lowered state, and more bound states will be created. The energy difference between the lowest bound state and the continuum, the so-called binding energy of the exciton state, will range from about 0.1 to 0.82 eV in a system with 30 unit cells within the parameter sets used in the current studies. When small electron-phonon coupling is taken into account, little further stabilization of the exciton state is achieved and the force constant K casts an insignificant effect on the binding energy. This can be shown from Eq. (13) that small lattice deformation makes the lattice energy not so important as the influence of electron-hole interaction. However, when $\beta = 0.4$, large enough for significant distortion of a relatively soft polymer backbone, extra binding energy of the exciton state can be gained, whereas the energies of almost all the other states, including the other bound states and the continuum, are a little higher than those of the preceding cases. This indicates that modest lattice relaxation mostly stabilizes the exciton state, i.e. the lowest bound state. We show these results in Fig. 2.

Since the wavefunction of the exciton state contains both the electron's and the hole's indices, we take two ways to observe its probability distribution. The diagonal, $|\Phi_{nn}|^2$, shows the distribution of the photo-generated electron-hole pair on the polymer, while the anti-diagonal, $|\Phi_{n,N+1-n}|^2$, reveals the average size of an exciton. We find that for weak electron-phonon coupling, the photoinduced charges are loosely linked and delocalized on the whole chain for a relative small U, but they pair up to form an exciton and are a little more probable to be found in the central region of a polymer if U is larger. On the other hand, for large electron-phonon coupling, the electron-hole pair is strongly bound and mostly locates at the central part for a soft lattice, whereas it falls back to the delocalized situation for a rigid lattice. It is clear that lattice relaxation helps the formation and localization of an exciton, and deflects the exciton state from the results calculated for a perfect lattice. In these cases V shows a smaller effect on the distribution and the size of an electron-hole pair than the on-site Coulomb interaction. Different chain length of a polymer is also considered, which shows the validity and generality of these results for a conducting polymer of a sufficient length (typically larger than 10 to 15 unit cells).

Displacement of each unit cell for different settings of parameters is shown in Fig. 3. We find that when $\beta = 0.01$ and 0.05, $K \cdot \Delta u_{n,EX}$ is almost the same curve for given U and V; it means if we fix β, U and V, the elastic force between adjacent unit cells is also fixed. Here the electron-hole interaction plays an important part in determining the degree of lattice distortion, but compared with the size of a unit cell, deformation is still very small. When $\beta = 0.1$ with K fixed, all $\Delta u_{n,EX}$ become very resemblant for different U and V, which shows the electron-phonon coupling gradually weighs more on the degree of lattice relaxation. In all of these cases the deformation is throughout the whole chain, clearly indicating the delocalized property of

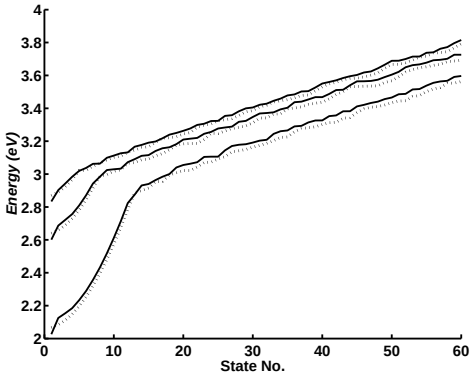

Figure 2: First 60 lowest states of the intrapolymer spectrum of a 30-unit polymer. For $U/(V/a_0) = 2$ and $K = 2.5$, the energies of the states are calculated for $\beta = 0$ (dotted line) and $\beta = 0.4$ (solid line) with different U, from the top pair to the bottom in the figure, equal to -0.5, -1 and -2. It is clear that the exciton state can be stabilized due to electron-phonon coupling, while almost the other states are on the contrary. In each case, the energy difference between the first two states is evidently much larger than that in the corresponding uncoupled case.

the photoinduced electron-hole pair. On the contrary, when $\beta = 0.4$ with K not too large, lattice distortion becomes larger and localized mainly within about 10 unit cells, and also favors the formation of a trapped exciton. All of the results are also checked with different numbers of unit cells, which shows the chain-length dependency is insignificant in our model.

In the aspect of the normal-mode analysis, the frequencies of normal modes are predominantly determined by the force constant K and are proportional to $\sqrt{K}$ if $\beta \leq 0.1$. In fact for β in this range, the lattice part of the system is close to $N - 1$ classical springs of the same force constant K in series, and the behavior of the normal modes and their frequencies can be one-to-one correlated to the results calculated by the classical mechanics. Different U, V and N (large enough) basically do not greatly affect these properties. However, if $\beta = 0.4$, long-wavelength phonon modes show significant contribution from the electron-hole excitation, which results in self-trapping, especially for the lattice with a small K. Thus larger electron-phonon coupling will make non-linear effects more pronounced in the system. Normal modes having centrally symmetric amplitudes will chiefly preserve their properties due to the maintenance of the localization of the electronic wavefunction, while some anti-symmetric low-frequency modes deviate from the classical results more, and the frequency order of neighboring modes may exchange. However, it can be shown that by the requirement of symmetry all anti-symmetric modes cannot contribute to the charge transfer, so this deviation will not severely affect our model. Normal modes of higher frequency still behave normally as the cases of weaker electron-phonon coupling, since the oscillation of their amplitudes largely cancels the correlation with the electronic wavefunction.

4.2 The Charge-transfer States

Now we come to the properties of the charge-transfer states, the electron having hopped onto the dopant and a single hole being left on the conducting polymer. There are N such states that can be calculated from the $N \times N$ Hamiltonian matrix, but we often cannot fulfill the self-consistent calculations of first two (six at most) highest states since the serious oscillation of the electronic probability amplitudes makes the adiabatic approximation and our strategy of calculation impractical when the electron-phonon coupling and the electron-hole interaction are both strong on a soft lattice. However, due to such oscillation which results in the extremely poor electronic correlations between these states and the exciton state, and due to the energy constraint for the acceptor level in the photoinduced charge-transfer study, such high-energy states can be safely omitted. In addition, the order of electronic states is retained throughout the iterations, thus tracking a certain wavefunction in our calculation is feasible, and the convergent outcome is proved confidential.

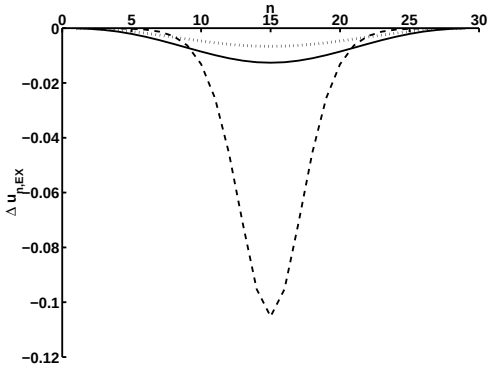

Figure 3: $\Delta u_{n,EX}$ for $U = -1$, $U/(V/a_0) = 2$, $K = 2.5$ and different β. Lattice deformation is small and throughout the whole chain when $\beta = 0.05$ (dotted line) and $\beta = 0.1$ (solid line), but much larger and confined within about 10 unit cells when $\beta = 0.4$ (dashed line).

In the charge-transfer spectrum the lowest state, namely the charge-transfer bound state, may evidently separate from the continuum (actually consisting of $N-1$ states). Compared with the energy distribution, a cosine function, of a long one-dimensional conjugated system in Hückel model, interaction between charges can bind the hole near the dopant and further lower the energy of this bound state, whose binding energy may be easily defined as the energy difference between the first two states. We find that when $\beta \leq 0.1$, the binding energy mainly depends on the effective distance of the molecule d and V/a_0. Moreover, it is approximately proportional to $|V|$ and d^{-1} if $d \geq 5$ and $|V/a_0| \geq 0.25$, which can be viewed from a classical picture as the potential energy between a hole in the center of a polymer and an electron on the molecule. If $|V|$ is too small, the system will be similar to Hückel model and there will be almost no binding energy. On the other hand, When $\beta = 0.4$, the effect of K will be noticeable, especially for the case of $K = 1$; in the meanwhile lattice relaxation helps stabilize the hole, thus extra binding energy is gained. Within the values chosen for the parameters, the binding energy of the bound state can be as large as 1 eV for extremely strong electron-phonon coupling, strong Coulomb interaction and soft lattice, or no more than 0.05 eV for the other extreme condition.

The hole wavefunctions of all the charge-transfer states are mainly determined by $|V/a_0|$. Charge localization in the bound state is explicit for strong electron-phonon interaction with the assistance of a soft backbone entering for weaker cases. In Fig. 4(a) we show the displacement of each unit cell in the charge-transfer bound state for different settings of parameters, and it is clear that the size of the hole-polaron is mainly related to the strength of Coulomb interaction; in Fig. 4(b) the displacements of some charge-transfer states are given, which indicates that lattice deformation is most evident in the bound state, while the "scattering" property is retained in the other states. Comparing the degree of deformation of these states with that of the exciton state, we should not neglect the effect of lattice relaxation in the exciton and the charge-transfer bound state, whether localized or delocalized. Size-dependence is still not important for all these results.

Similar to the discussion in the last subsection, the normal modes and their frequencies of most CT states are approximately of the classical behavior (see Fig. 5). Larger deviation will appear in higher states and in the cases of strong electron-phonon coupling in a very soft lattice. However, from the viewpoint of approximation, the deviation will not seriously affect the basic assumptions of our model, and therefore the calculation of the decay rate will still be applicable.

4.3 The Charge-transfer Rate

From Eq. (1) we know that the charge-transfer states, with energies $E_{polymer,CTm}$ higher than $E_{EX} + E_{polymer,CT1}$, will not be an energetically-favored decay path, thus can be excluded from the computation of the transfer rate. This elimination is also beneficial for our model, since only those well-behaved final

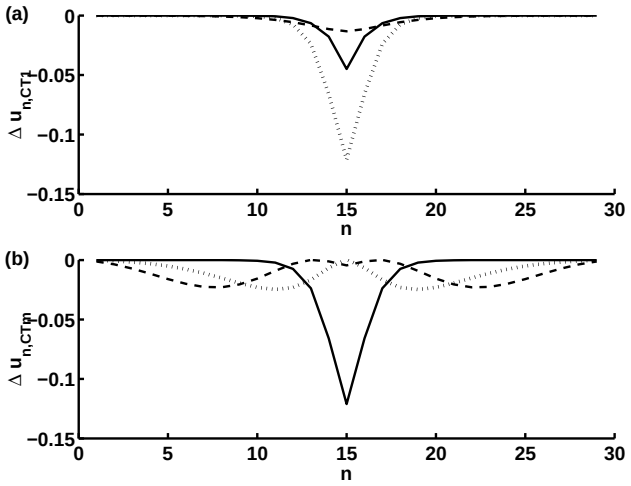

Figure 4: (a) For $K = 2.5$, $\Delta u_{n,CT1}$ for $\beta = 0.1$, $V/a_0 = -0.25$, $d = 7.5$ (dashed line), for $\beta = 0.1$, $V/a_0 = -0.5$, $d = 2.5$ (solid line), and for $\beta = 0.4$, $V/a_0 = -0.5$, $d = 2.5$ (dotted line). Lattice deformation is large for stronger electron-phonon coupling. (b) $\Delta u_{n,CTm}$ for $\beta = 0.4$, $V/a_0 = -0.5$ and $d = 2.5$ when $m = 1$ (solid line), $m = 2$ (dotted line), and $m = 3$ (dashed line). Lattice distortion is small and throughout the whole chain for all the other charge-transfer states except the bound state.

states will be considered. Examining the electronic correlations $\langle \Psi_{CTm}|\mathcal{V}_i|\Psi_{EX}\rangle_0$ in Eq. (19), we summarize some features as the following. First, the electronic matrix elements between the exciton state and the $2m$th antisymmetric charge-transfer states will vanish. Second, for $\beta \leq 0.1$ and $d \geq 5$, different settings of the parameters have a minor effect on the magnitude of $\langle \Psi_{CT1}|\mathcal{V}_1|\Psi_{EX}\rangle_0$, but smaller $|U|$ and larger $|V|$ disadvantage the other single-particle hopping channels. It is probable that this mechanism of charge transfer will be more favorable for situations with more concentrated charge density near the molecule in the initial state and less electron-hole attraction in the final state. Because of the inphase wavefunction of the charge-transfer bound state, the magnitude of the matrix element, $|\langle \Psi_{CT1}|\mathcal{V}_1|\Psi_{EX}\rangle_0|$, will be one to two orders of magnitude larger than the other matrix elements of $\mathcal{V}_1$ (see Eq. (20)). Third, $\langle \Psi_{CTm}|\mathcal{V}_2|\Psi_{EX}\rangle_0$ depends relatively little on the strength of electron-hole interaction and the final states; from Eq. (21) we can see that it is because the amplitudes of final CT-states have a similar order of magnitudes in the vicinity of the dopant. However, $|\langle \Psi_{CT1}|\mathcal{V}_2|\Psi_{EX}\rangle_0|$ is still the largest. Fourth, when $\beta = 0.4$, lattice relaxation will help localize the charges, and a softer lattice will make the matrix elements of $\mathcal{V}_1$ and $\mathcal{V}_2$ larger (see Fig. 6). Fifth, for some final states cancellation may occur if the two perturbations are of comparable orders of magnitude, since at this time $\langle \Psi_{CTm}|\mathcal{V}_1|\Psi_{EX}\rangle_0$ and $\langle \Psi_{CTm}|\mathcal{V}_2|\Psi_{EX}\rangle_0$ are occasionally of similar magnitudes but of opposite signs. Therefore it may not be suitable to separately deal with the two decay processes to calculate the overall rate. Compared with the previous research, the electronic correlations between the excitonic and charge-transfer bound states are found to be the most efficient, so it is necessary to take this decay route into consideration.

In the computation of Huang-Rhys factors (see Eq. (18)), the displacement of equilibrium δ_{n_i} along the nth normal mode is calculated by the difference between the inner products of the mass-weighted normal-mode amplitudes and the lattice displacements of the initial and the final states, respectively. By the symmetry argument we know that the inner products concerning one half of the modes vanish, so they will not contribute to the rate. On the other hand, we find that the meaningful mode of lowest frequency is the most significant contributor to the sum of all Huang-Rhys factors, and for higher final states this sum also becomes larger. In Table 2 we show the ranges of the sums for different magnitude of the electron-hole interaction with respect to different β and K. It is clearly shown that our parameter settings cover from the cases of weak electron-phonon coupling (the lower-left corner) to those of strong coupling (the upper-right corner). Eq. (19) is therefore applicable to calculate the charge-transfer rate for the conditions of the

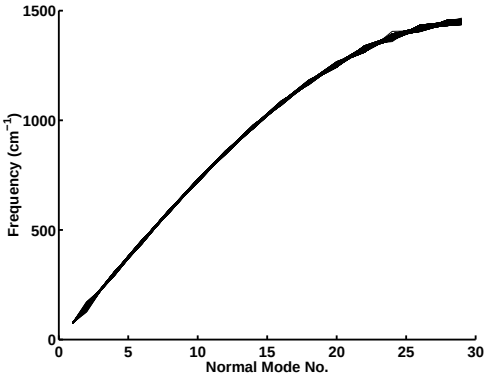

Figure 5: The frequencies of all normal modes of first 20 charge-transfer states for $\beta = 0.4$, $K = 5$ and different strength of electron-hole interaction for $N = 30$. Small deviation from the classical behavior appears in higher charge-transfer states.

Table 2: The ranges of the sums of all Huang-Rhys factors for different β and K. Each range contains the outcome of different settings of the other parameters, where the lower bound is obtained from the data about the charge-transfer bound state, the upper bound from the data about a higher final state.

$\sum_i S_{n_i}$	$\beta = 0.01$	$\beta = 0.05$	$\beta = 0.1$	$\beta = 0.4$
K=1	$0.02 - 0.18$	$0.3 - 2.4$	$1.3 - 8.2$	$30 - 180$
K=2.5	$0.005 - 0.045$	$0.1 - 0.6$	$0.32 - 1.95$	$6 - 40$
K=5	$0.002 - 0.016$	$0.03 - 0.21$	$0.11 - 0.68$	$2 - 11.5$
K=10	$0.0005 - 0.0058$	$0.001 - 0.075$	$0.04 - 0.24$	$0.5 - 3.6$

upper-right corner.

Now we evaluate the time scale in which the charge transfer takes place. We find that the decay to the bound state is about two orders of magnitude faster than the other decay paths; the former may even arise within a subpicosecond time scale for the weak perturbations t_0 and v_0 (about 0.001 to 0.01 eV), whereas the latter may also occur in a similar time measure for moderate t_0 and v_0 (about 0.1 eV) in zero temperature. In addition, the rates of the latter cases will fall off as N becomes larger since the electronic wavefunctions of the final states have the property of "scattering", but the rate of the former channel is nearly chain-length independent due to charge localization, which belongs to an ultrafast photoinduced charge-transfer process. Because of the small Huang-Rhys factors, this rate will not be seriously affected by higher temperature, but the energy requirement of Δ is relatively sharp. Fig. 7 shows the decay rate in 80 K for $\beta = 0.4$, $U = -1$, $U/(V/a_0) = 2$, $d = 5$ and $K = 2.5$.

5 Discussion

We have successfully established a lattice relaxation theory of photoinduced charge transfer in a conjugated polymer/dopant composite, and discussed the applicability of our model and the roles of many parameters in detail. State-to-state charge-transfer rates can be estimated readily, and creation of phonons conserved the energy in the decay process. Charge transfer may take place from the initial bound state to the final bound one within $10^{-13} - 10^{-14}$ second under weak perturbations, which shows the charge-transfer to the bound CT exciton is much more effective than to the CT-continuum. As recent experimental data revealed,[11] very fast time constant was observed, so detailed first-principle calculations to determine the relative energies of important states and bands in the polymer/dopant composite may help clarify which kind of decay path is taken in such an ultrafast process. However, we here suggest that the synthesis of a composite in which photoinduced charge transfer from the excitonic bound state to the localized polaron state is accomplishable may fabricate a system capable of fastest and most efficient photogenerated charge

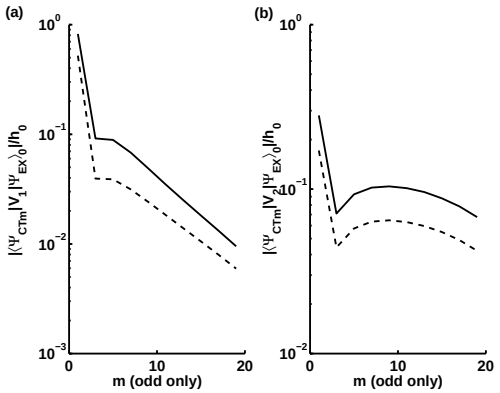

Figure 6: For $N = 30$, (a) $|\langle\Psi_{CTm}|\mathcal{V}_1|\Psi_{EX}\rangle_0|/h_0$ and (b) $|\langle\Psi_{CTm}|\mathcal{V}_2|\Psi_{EX}\rangle_0|/v_0$ plotted versus odd m only. In each subplot, the dashed line is corresponding to the case of $\beta = 0.1$, and the solid is to the case of $\beta = 0.4$ for $U = -2$, $U/(V/a_0) = 4$, $d = 5$, and $K = 2.5$. It can be seen that as the energy of the final state goes higher, the matrix element of $\mathcal{V}_1$ reduces more but that of $\mathcal{V}_2$ variates slightly, which coincides with the work of Rice and Gartstein.[17] However, we show that the charge-transfer bound state is more important as the final state, and lattice relaxation may further encourage the electronic correlations and therefore the charge transfer.

separation.

From our calculations, it is found that for localized excitations the polymer-size and the temperature dependence of the transfer rate will nearly vanish, and with our choices for the parameters, the size of a localized exciton or polaron will be about $5 - 10$ unit cells. If local excitation on the polymer chain is the primary event in the initial stage and a dopant molecule is in its vicinity, weak perturbations can efficiently quench the exciton and separate the electron-hole pair. In our theory, the introduction of the dopant concentration factor is not required, and for the cases of different doping levels, the generalization to a conducting polymer with multiple molecules is also applicable. We believe that the relation between the calculated rate and the dopant concentration will be more reasonable and able to approximately reflect the real situations.

In this paper we consider the electron-phonon coupling off-diagonally, so basically only acoustic phonons are concerned in our model. Because of their low frequencies, creation of phonons to conserve the energy confine the acceptor level on the molecule within several discrete ranges (see Fig. 7). We notice that the frequencies of important vibrational oscillations of conducting polymers are often more than 1000 cm^{-1},[11] close to the behavior of optical phonons. As mentioned in the beginning of Sec. 3, site-diagonal coupling could also be an important contribution to the lattice relaxation on the photogeneration process. Results of this mechanism will be presented lately.

From the derivation of the microscopic Hamiltonian we find some terms that can distinguish singlet and triplet systems, thus studying the differences of their photophysics is feasible. It is also possible to extend our model to study charge separation or recombination between two identical polymer chains of different spatial orientations or between two different kinds of polymers. Aspects of these problems are under research.

acknowledgements: This research was supported by the National Science Council, Republic of China (Grant No. NSC90-2113-M-002-056).

References

[1] N. S. Sariciftci, L. Smilowitz, A. J. Heeger, and F. Wudl. *Science*, 258:1474, 1992.

[2] S. Morita, A. A. Zakhidov, and K. Yoshino. *Solid State Commun.*, 82:249, 1992.

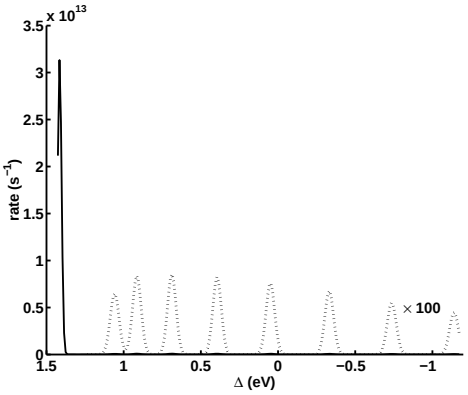

Figure 7: The charge-transfer rate in 80 K for $\beta = 0.4$, $U = -1$, $U/(V/a_0) = 2$, $d = 5$ and $K = 2.5$ with respect to the energy of the acceptor level of the molecule. Here t_0 and v_0 are taken to be 0.01 eV. 100 times the original data are shown in the dotted line for detail.

[3] B. Kraabel, C. H. Lee, D. McBranch, D. Moses, N. S. Sariciftci, and A. J. Heeger. *Chem. Phys. Lett.*, 213:389, 1993.

[4] L. Smilowitz, N. S. Sariciftci, R. Wu, C. Gettinger, A. J. Heeger, and F. Wudl. *Phys. Rev. B*, 47:13835, 1993.

[5] K. H. Lee, René A. J. Janssen, N. S. Sariciftci, and A. J. Heeger. *Phys. Rev. B*, 49:5781, 1994.

[6] René A. J. Janssen, D. Moses, and N. S. Sariciftci. *J. Chem. Phys.*, 101:9519, 1994.

[7] B. Kraabel, D. McBranch, N. S. Sariciftci, D. Moses, and A. J. Heeger. *Phys. Rev. B*, 50:18543, 1994.

[8] René A. J. Janssen, Jan C. Hummelen, K. Lee, K. Pakbaz, N. S. Sariciftci, A. J. Heeger, and F. Wudl. *J. Chem. Phys.*, 103:788, 1995.

[9] B. Kraabel, Jan C. Hummelen, D. Vacar, D. Moses, N. S. Sariciftci, and A. J. Heeger. *J. Chem. Phys.*, 104:4267, 1996.

[10] S. V. Frolov, P. A. Lane, M. Ozaki, K. Yoshino, and Z. V. Vardeny. *Chem. Phys. Lett.*, 286:21, 1998.

[11] C. J. Brabec, G. Zerza, G. Cerullo, S. de Silvestri, S. Luzzati, J. C. Hummelen, and N. S. Sariciftci. Tracing photoinduced electron transfer process in conjugated polymer/fullerene bulk heterojunctions in real time. *Chem. Phys. Lett.*, 340:232, 2001.

[12] J. J. M. Halls, C. A. Walsh, N. C. Greenham, E. A. Marseglia, R. H. Friend, S. C. Moratti, and A. B. Holmes. *Nature*, 376:498, 1995.

[13] G. Yu, J. Gao, J. C. Hummelen, F. Wudl, and A. J. Heeger. *Science*, 270:1789, 1995.

[14] N. S. Sariciftci. *Prog. Quant. Electr.*, 19:131, 1995.

[15] K. Yoshino, S. Lee, A. Fujii, H. Nakayama, W. Schneider, A. Naka, and M. Ishikawa. *Adv. Mater.*, 11:1382, 1999.

[16] C. J. Brabec and N. S. Saricifci. *Monatshefte für Chemie*, 132:421, 2001.

[17] M. J. Rice and Yu. N. Gartstein. Theory of photoinduced charge transfer in a molecularly doped conjugated polymer. *Phys. Rev. B*, 53(16):10764, 1996.

[18] K. Huang and A. Rhys. *Proc. Roy. Soc. London, Ser. A*, 204:406, 1951.

[19] S. H. Lin, R. Alden, R. Islampour, H. Ma, and A. A. Villaeys. *Density Matrix Method and Femtosecond Processes*. World Scientific, Singapore, 1991.

[20] H. Haken. *Quantum Field Theory of Solids: An Introduction*. North-Holland, Amsterdam, 1976.

[21] L. I. Schiff. *Quantum Mechanics*. McGraw-Hill, Singapore, third edition, 1968.